 CMES, vol.53, no.1, pp.1-22, 2009

A Dual Hybrid Boundary Node Method for 2D Elastodynamics Problems

Yu Miao[1], Qiao Wang[1], Bihai Liao[1,2] and Junjie Zheng[1]

Abstract: As a truly meshless method, the Hybrid Boundary Node method (Hybrid BNM) does not require a 'boundary element mesh', either for the purpose of interpolation of the solution variables or for the integration of 'energy'. This paper presents a further development of the Hybrid BNM to the 2D elastodynamics. Based on the radial basis function (RBF) and the Hybrid BNM, it presents an inherently meshless, boundary-only technique, which named dual hybrid boundary node method (DHBNM), for solving 2D elastodynamics. In this study, the RBFs are employed to approximate the inhomogeneous terms via dual reciprocity method (DRM), while the general solution is solved by means of Hybrid BNM, in which only requires discrete nodes constructed on the boundary of a domain, several nodes in the domain are needed just for the RBF interpolation. The rigid body movement method is employed to solve the hypersingular integrations. The 'boundary layer effect', which is the main drawback of the original Hybrid BNM, has been circumvented by an adaptive integration scheme. The computation results obtained by the present method are shown that high convergence and high accuracy with a small node number are achievable.

Keywords: Hybrid boundary node method; Dual reciprocity method; Radial basis function; 2D elastodynamics

1 Introduction

Structural dynamic analysis is one of the main required tasks for an engineer to accomplish in the analysis of buildings. Many numerical methods are available in this field such as the finite element method (FEM) (Zienkiewicz, 1977), which has some disadvantages such as: the need for discretizing the entire problem domain,

[1] School of Civil Engineering and Mechanics, Huazhong University of Science and Technology, Wuhan 430074, China

[2] Corresponding author. Tel: +8627-87540233; Fax: +8627-87542231; Email: shangha9459@163.com

and the inaccuracies in cases of stress concentration. The boundary element method (BEM) (Brebbia and Dominguez, 1992), has been used to overcome these problems since it only requires the discretization of the boundary and produces excellent results for stress concentration cases. BEM can also offer easy solution for complex structures in less time and higher accuracy. However, BEM still uses elements to implement both interpolation and integration. In case of large deformation, moving boundary problems, the elements may be heavily distorted, thus the shape functions based on elements could be of poor properties.

In the recent years, meshless methods have attracted much attention due to their flexibility, and absolutely no elements or cells are needed in the present formulation, either for interpolation purposes or for integration purposes. According to the way of the discretization, the meshless methods can be roughly grouped into two categories, namely domain type methods and boundary type methods. For the former, there are the diffuse element method (DEM) (Nayroles et.al., 1992), the element free Galerkin (EFG) method (Belytschko et.al., 1994), the reproducing Kernel particle method (RKPM) (Liu et.al., 1996),the point interpolation method (PIM) (Liu and Gu, 2001), the meshless local Petrov–Galerkin method(MLPG) (Atluri and Zhu, 1996), the local point interpolation method(LPIM) (Gu and Liu, 2001) , the method of finite spheres(MFS) (De and Bathe, 2001), the finite cloud method (FCM) (Aluru and Li, 2001) and so on. For the latter, there are the local boundary integral equation method(LBIM) (Zhu, 1999), the boundary node method(BNM) (Mukherjee and Mukherjee, 1999), the boundary only radial basis function method (BRBFM) (Cheri and Tanaka, 2002), the boundary point interpolation method (BPIM) (Liu, 2002), and the hybrid boundary node method(Hybrid BNM) (Zhang, 2002; Miao, 2005).

The Hybrid BNM gets rid of the background elements and achieves a truly boundary–type meshless method. It uses the moving least squares to approximate the boundary solution variables, and the integration is limited to a fixed local region on the boundary. No elements are needed either for interpolate or for integration, and at the same time it has the advantage of dimensionality reduction. It has been applied to the potential problems (Zhang, 2003; Miao, 2009) and elasticity problems (Miao, 2006; Miao, 2005).However, like the BEM, it is not convenient for solving elastodynamic analysis in the frequency or time domain because applying the elastodynamic fundamental solution increases the computational effort and the domain integration is inevitable. In BEM, to overcome these drawbacks, Nardini and Brebbia (1982) and Nardini and Brebbia (1985) developed a new formulation, which is named the dual reciprocity method (DRM). In the DRM, the integral equation of the body is presented in terms of its boundary variables and includes a domain integral corresponding to the body inertia forces. This integral can be transformed to the

boundary using a new collocation scheme to approximate the field accelerations, or consequently the field displacements.

In this paper, a truly meshless methodÂ£ÂDual Hybrid Boundary Node method (DHBNM), has been developed and applied for elastodynamic problems. The method is formed by combining Hybrid BNM with DRM. In this method, the solutions are divided into two parts: complementary solution and particular solution. For the former, as the same to Hybrid BNM, the variables inside the domain are interpolated by the fundamental solution while the boundary unknown variables are approximated by moving least square approximation (MLS) (Lancaster and Salkauskas, 1981). The modified variational formulation is applied to form the discrete equations of hybrid boundary node method. For the latter, the DRM has been employed, and applies radial basis function (RBF) to interpolate the inhomogeneous part of the equation. Because of the acceleration term of the governing equation, the boundary integral equations obtained by DHBNM is not enough to solve all solution variables, some additional equations are proposed to obtain the connection of the variables in the domain and on the boundary. In this method, they are obtained by interpolation of the fundamental solution and the basis form of the particular solution. In order to overcome singular integration, rigid body moving method has been applied. Numerical examples presented in this paper for the solution of elastodynamic problems are studied to demonstrate the validity and accuracy of the proposed formulation.

The discussions of this method are arranged as following: the review of the Hybrid BNM will be discussed in section 2. The DHBNM for elastodynamic problems is developed in section 3. Additional equations and final system equation will be formed in section 4. Numerical examples for elastodynamic problems are shown in section 5. Finally, the paper will end with conclusion in section 6.

2 Review of the Hybrid BNM

This section gives a brief review of the Hybrid BNM. For convenience, the governing equation for the structure dynamics is

$$\sigma_{ij,j} + b_i = c\dot{u}_i + \rho\ddot{u}_i \tag{1}$$

Where ρ is density of the material and c is the damping coefficient. $\ddot{u}_i = \partial^2 u_i/\partial t^2$ and $\dot{u}_i = \partial u_i/\partial t$. σ_{ij} is the stress tensor corresponding to the displacement field u_i, b_i is the body force, and $()_{,j}$ denotes $\partial()/\partial x_j$.

The corresponding boundary and initial conditions are given as follows:

$$u_i = \bar{u}_i \text{ on the essential boundary } \Gamma_u, \tag{2}$$

$$\sigma_{ij} \cdot n_j = \bar{t}_i \text{ on the natural boundary } \Gamma_t, \tag{3}$$

$$u(x,t_0) = u_0(x), \tag{4}$$

$$\dot{u}(x,t_0) = v_0(x), \tag{5}$$

Where $\bar{u}_i$ and $\bar{t}_i$ are the prescribed displacements and tractions, respectively. u_0 and v_0 are the initial displacements and velocities at the initial time t_0 respectively. n_j is the unit outward normal to the boundary $\Gamma(\Gamma = \Gamma_u + \Gamma_t)$.

For convenience, c and b_i are set equal to zero, the governing equation for the elastodynamics without damping is rewritten as

$$\sigma_{ij,j} = \rho \ddot{u}_i \tag{6}$$

From the equations above, one can obtain two second-order partial differential equations for displacement components. The result can be written in the form

$$G u_{i'kk} + \frac{G}{1-2\nu} u_{k'ki} = \rho \ddot{u}_i \tag{7}$$

where $G = \frac{E}{2(1+\nu)}$ is shear modulus, and ν is Poisson ratio.

As a consequence, the left-hand side of Eq.(7) can be dealt with by Hybrid BNM for the Laplace equation, and the integrals corresponding to the right-hand side are taken to the boundary using DRM. In dual hybrid boundary node method (DHBNM), the solution variables u can be divided into complementary solutions u^c and particular solutions u^p, i.e.

$$u = u^c + u^p \tag{8}$$

The particular solution u^p just needs to satisfy the inhomogeneous equation as follow:

$$G u^p_{i'kk} + \frac{G}{1-2\nu} u^p_{k,ki} = \rho \ddot{u}_i \tag{9}$$

The complementary solution u^c must satisfy the Laplace equation and the modified boundary condition, so they can be written in the form

$$G u^c_{i'kk} + \frac{G}{1-2\nu} u^c_{k,ki} = 0 \tag{10}$$

$$u^c = \bar{u}^c = \bar{u} - u^p \tag{11}$$

$$t^c = \bar{t}^c = \bar{t} - t^p \tag{12}$$

In the following, the complementary solution will be solved by the Hybrid BNM. The Hybrid BNM is based on a modified variational principle. The functions in the modified principle assumed to be independent are: displacement field within the domain, u, boundary displacement field $\tilde{u}$ and boundary traction $\tilde{t}$. Consider a domain Ω enclosed by $\Gamma = \Gamma_u + \Gamma_t$ with prescribed displacement $\bar{u}$ and traction $\bar{t}$ at the boundary portions Γ_u and Γ_t, respectively. The corresponding variational function Π_{AB} is defined as [19,20]

$$\Pi_{AB} = \int_{\Omega} \frac{1}{2} u_{,i} u_{,i} d\Omega - \int_{\Gamma} \tilde{t}\,(u-\tilde{u})\, d\Gamma - \int_{\Gamma_t} \bar{t}\tilde{u} d\Gamma \tag{13}$$

where, the boundary displacement $\tilde{u}$ satisfies the essential boundary condition, i.e. $\bar{u} = \tilde{u}$, on Γ_u.

With the vanishing of $\delta\Pi_{AB}$ over the domain and its boundary, the following equivalent integral can be obtained

$$\int_{\Gamma} (t-\tilde{t}) \delta\tilde{u} d\Gamma - \int_{\Omega} u_{,ii} \delta\tilde{u} d\Omega = 0 \tag{14}$$

$$\int_{\Gamma} (u-\tilde{u}) \delta\tilde{t} d\Gamma = 0 \tag{15}$$

$$\int_{\Gamma_t} (\tilde{t}-\bar{t}) \delta\tilde{u} d\Gamma = 0 \tag{16}$$

Eq. (16) will be satisfied if the traction boundary condition, $\tilde{t} = \bar{t}$, is imposed. So it would be ignored in the following.

Eq. (14) and (15) hold for any portion of the domain Ω, for example, a sub-domain Ω_s, defined as an intersection of a domain and a small circle centered at node $S_I^{[11]}$, and its boundary Γ_s and L_s. (see Fig.1).

We use the following weak form for the sub-domain and its boundary to replace Eq. (14) and (15)

$$\int_{\Gamma_s + L_s} (t-\tilde{t}_s) h d\Gamma - \int_{\Omega_s} u_{,ii} h d\Omega = 0 \tag{17}$$

$$\int_{\Gamma_s + L_s} (u-\tilde{u}_s)\, h d\Gamma = 0 \tag{18}$$

where h is a test function. We approximate $\tilde{u}_s$ and $\tilde{t}_s$ at the boundary Γ by the moving least square (MLS) approximation, as

$$\tilde{u}(s) = \sum_{I=1}^{N} \Phi_I(s) \hat{u}_I \tag{19}$$

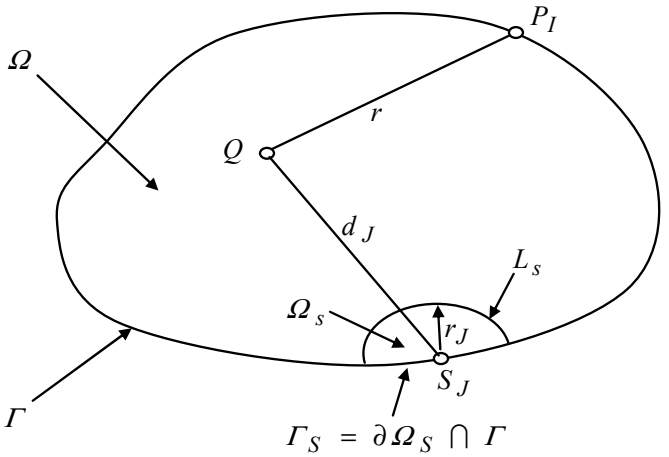

Figure 1: Local domain and source point of fundamental solution corresponding to S_J.

$$\tilde{t}(s) = \sum_{I=1}^{N} \Phi_I(s)\hat{t}_I \tag{20}$$

where N stands for the number of nodes located on the surface; $\hat{u}_I$ and $\hat{t}_I$ are nodal values, and $\Phi_I(s)$ is the shape function of the MLS approximation, corresponding to node S_I, which is given by

$$\Phi_I(s) = \sum_{j=1}^{m} p_j(s)\left[A^{-1}(s)B(s)\right]_{jI} \tag{21}$$

In the above equation, $p_j(s)$ provide a basis of order m. In this study, we take m to 3, namely, $\mathbf{p}^{\mathrm{T}}(\mathbf{s}) = \begin{bmatrix}1, & s, & s^2\end{bmatrix}$. Matrixes $A(\mathbf{s})$ and $B(\mathbf{s})$ are defined as

$$A(s) = \sum_{I=1}^{N} w_i(s)\mathrm{p}(s_I)\,\mathrm{p}^{\mathrm{T}}(s_I) \tag{22}$$

$$B(s) = [w_1(s)p(s_1), w_2(s)p(s_2), \ldots w_N(s)p(s_N)] \tag{23}$$

In Eq.(22) and (23), $w_I(s)$ are weight functions. Gaussian weight function corresponding to node s_I can be written as

$$w_I(s) = \begin{cases} \dfrac{\exp\left[-(d_I/c_I)^2\right]-\exp\left[-\left(\hat{d}_I/c_I\right)^2\right]}{1-\exp\left[-\left(\hat{d}_I/c_I\right)^2\right]}, & 0 \le d_J \le \hat{d}_I \\ 0 & d_J \ge \hat{d}_I \end{cases} \tag{24}$$

where $d_I = |s - s_I|$ is the distance between an evaluation point and node s_I, c_I is a constant controlling the shape of the weight function w_I and $\hat{d}_I$ is the size of the support for the weight function w_I and determines the support of node s_I.

In Eqs.(17) and (18), $\tilde{u}_s$ and $\tilde{t}_s$ at Γ_s can be represented by $\tilde{u}$ and $\tilde{t}$ expressed in Eq.(19) and (20) since Γ_s is a portion of Γ, while $\tilde{u}_s$ and $\tilde{t}_s$ at L_s has not been defined yet. To solve this problem, we select h such that all integrals vanish overL_s. This can be easily accomplished by using the weight function in the MLS approximation for h, with the half-length of the major axis d_I of the support of the weight function being replaced by the radius of the sub-domainΩ_s, i.e.

$$h_J(Q) = \begin{cases} \frac{\exp\left[-(d_J/c_J)^2\right] - \exp\left[-(r_J/c_J)^2\right]}{1 - \exp\left[-(r_J/c_J)^2\right]}, & 0 \le d_J \le r_J \\ 0, & d_J \ge r_J \end{cases} \tag{25}$$

where d_J is the distance between point Q in the domain and the nodal point s_J. Therefore, $h_J(Q)$ vanishes on L_s. Eq.(17) and (18) can be rewritten as

$$\int_{\Gamma_s} (t - \tilde{t}) h d\Gamma - \int_{\Omega_s} u_{,ii} h d\Omega = 0 \tag{26}$$

$$\int_{\Gamma_s} (u - \tilde{u}) h d\Gamma = 0 \tag{27}$$

Making use of fundamental solutions, we approximate u inside the domain by

$$\mathbf{u} = \begin{Bmatrix} u_1 \\ u_2 \end{Bmatrix} = \sum_{I=1}^{N} \begin{bmatrix} u_{11}^I & u_{12}^I \\ u_{21}^I & u_{22}^I \end{bmatrix} \begin{Bmatrix} x_1^I \\ x_2^I \end{Bmatrix} \tag{28}$$

and hence at a boundary node, the normal flux is given by

$$\mathbf{t} = \begin{Bmatrix} t_1 \\ t_2 \end{Bmatrix} = \sum_{I=1}^{N} \begin{bmatrix} t_{11}^I & t_{12}^I \\ t_{21}^I & t_{22}^I \end{bmatrix} \begin{Bmatrix} x_1^I \\ x_2^I \end{Bmatrix} \tag{29}$$

where u_I^s is the fundamental solution; x_I are unknown parameters; N is the total number of boundary nodes. The fundamental solution is written as[2]

$$u_{ij}^I = \frac{-1}{8\pi(1-\nu)G} \left[(3 - 4\nu) \delta_{ij} \ln(r) - r_{,i} r_{,j} \right] \tag{30}$$

$$t_{ij}^I = \frac{-1}{4\pi(1-\nu)r} \left\{ \left[(1 - 2\nu) \delta_{ij} + 2 r_{,i} r_{,j} \right] \frac{\partial r}{\partial n} + (1 - 2\nu) \left(r_{,i} n_j - r_{,j} n_i \right) \right\} \tag{31}$$

Where δ is the Kronecker delta function, r is the distance between the source point and the field point, n is the normal to the boundary.

From the fundamental solution of the traction t, one can see it contains $(1/r)$ type singular integral. And it is obvious that the second term of Eq. (17) only attributes to the principal diagonal of the matrix. Hence, it can be treated by the rigid body movement method together with the singular integrals. So the final equations can be obtained as

$$\sum_{I=1}^{N_t} \int_{\Gamma_S} \begin{bmatrix} t_{11}^I & t_{12}^I \\ t_{21}^I & t_{22}^I \end{bmatrix} \begin{Bmatrix} x_1^I \\ x_2^I \end{Bmatrix} h_J(Q) d\Gamma = \sum_{I=1}^{N_t} \int_{\Gamma_S} \begin{bmatrix} \Phi_I(s) & 0 \\ 0 & \Phi_I(s) \end{bmatrix} \begin{Bmatrix} \hat{t}_1^I \\ \hat{t}_2^I \end{Bmatrix} h_J(Q) d\Gamma \tag{32}$$

$$\sum_{I=1}^{N_t} \int_{\Gamma_S} \begin{bmatrix} u_{11}^I & u_{12}^I \\ u_{21}^I & u_{22}^I \end{bmatrix} \begin{Bmatrix} x_1^I \\ x_2^I \end{Bmatrix} h_J(Q) d\Gamma = \sum_{I=1}^{N_t} \int_{\Gamma_S} \begin{bmatrix} \Phi_I(s) & 0 \\ 0 & \Phi_I(s) \end{bmatrix} \begin{Bmatrix} \hat{u}_1^I \\ \hat{u}_2^I \end{Bmatrix} h_J(Q) d\Gamma \tag{33}$$

Using the above equations for all nodes, one can get the system equations

$$\mathbf{Tx} = \mathbf{H}\hat{\mathbf{t}}^c \tag{34}$$

$$\mathbf{Ux} = \mathbf{H}\hat{\mathbf{u}}^c \tag{35}$$

where

$$U_{IJ} = \int_{\Gamma_s} \begin{bmatrix} u_{11}^I & u_{12}^I \\ u_{21}^I & u_{22}^I \end{bmatrix} h_J(Q) d\Gamma \tag{36}$$

$$T_{IJ} = \int_{\Gamma_s} \begin{bmatrix} t_{11}^I & t_{12}^I \\ t_{21}^I & t_{22}^I \end{bmatrix} h_J(Q) d\Gamma \tag{37}$$

$$H_{IJ} = \int_{\Gamma_s} \begin{bmatrix} \Phi_I(s) & 0 \\ 0 & \Phi_I(s) \end{bmatrix} h_J(Q) d\Gamma \tag{38}$$

3 DHBNM for elastodynamics

As an extension of the Hybrid BNM, the main idea of the DHBNM consists of employing the fundamental solution corresponding to a simpler equation and considering the remaining terms of the original equation via a procedure which involves a series expansion using RBF and the reciprocity principles. In the past sections, the complementary solution has been solved successfully by Hybrid BNM, in this section, the DRM will be developed to solve the particular solution.

3.1 Dual Reciprocity Method (DRM)

The DRM can be used in elastodynamic problems to transform the domain integral arising from the application of inhomogeneous into equivalent boundary integrals. Applying interpolation for inhomogeneous term, the following approximation can

be proposed for the term: $\rho\ddot{u}_i$ (Kontoni and Beskos, 1993; Samaan and Rashed, 2007)

$$\rho\ddot{u}_i \approx \sum_{j=1}^{N+L} f^j a_i^j \tag{39}$$

where the a_i^j are a set of initially unknown coefficients, the f^j are approximation functions. N and L are the total number of boundary nodes and total number of interior nodes respectively.

As the same of the Eq.(39), the particular solution can be approximated by the basis form of the particular solutions. It can be written as following

$$u_i^p \approx \sum_{j=1}^{N+L} \alpha_l^j \bar{\bar{u}}_{li}^j \tag{40}$$

If u^p satisfies Eq.(9), the following equations can be obtained

$$G\bar{\bar{u}}_{mk,ll}^j + \frac{G}{1-2\nu}\bar{\bar{u}}_{lk,lm}^j = \delta_{mk} f^j \tag{41}$$

The approximation function, f^j, can be chosen as $f^j = 1 + r$. Obviously, the basis form of particular solution $\bar{\bar{u}}$ satisfying Eq.(41) can be obtained as

$$\bar{u}_{km} = \frac{1-2\nu}{(5-4\nu)G} r_{,m} r_{,k} r^2 + \frac{1}{30(1-\nu)G}\left[\left(3 - \frac{10\nu}{3}\right)\delta_{mk} - r_{,m} r_{,k}\right] r^3 \tag{42}$$

The corresponding expression for the traction $\bar{\bar{t}}$ is

$$\begin{aligned} \bar{t}_{km} = {} & \frac{2(1-2\nu)}{(5-4\nu)}\left[\frac{1+\nu}{1-2\nu} r_{,m} r_{,k} + \frac{1}{2} r_{,k} n_{,m} + \frac{1}{2}\delta_{mk}\frac{\partial r}{\partial n}\right] r + \\ & \frac{1}{15(1-\nu)}\left[(4-5\nu)\, r_{,k} n_m - (1-5\nu)\, r_{,m} n_k + \left[(4-5\nu)\,\delta_{mk} - r_{,m} r_{,k}\right]\frac{\partial r}{\partial n}\right] r^2 \end{aligned} \tag{43}$$

And the particular solution of the stress can be given as

$$\begin{aligned} \bar{\sigma}_{lkm} = {} & \frac{2(1-2\nu)}{5-4\nu}\left[\frac{1+\nu}{1-2\nu}\delta_{kl} r_{,m} + \frac{1}{2}\left(\delta_{mk} r_{,l} + \delta_{ml} r_{,k}\right)\right] r + \\ & \frac{1}{15(1-\nu)}\left[(4-5\nu)\left(\delta_{mk} r_{,l} + \delta_{ml} r_{,k}\right) - (1-5\nu)\,\delta_{kl} r_{,m} - r_{,m} r_{,k} r_{,l}\right] r^2 \end{aligned} \tag{44}$$

Solving the Eqs. (40) , (42) and (43), particular solutions can be written as

$$u_i^p = \sum_{I=1}^{N+L} \begin{bmatrix} \bar{u}_{11}^I & \bar{u}_{12}^I \\ \bar{u}_{21}^I & \bar{u}_{22}^I \end{bmatrix} \begin{Bmatrix} \alpha_1^I \\ \alpha_2^I \end{Bmatrix} \tag{45}$$

$$t_i^p = \sum_{I=1}^{N+L} \begin{bmatrix} \bar{t}_{11}^I & \bar{t}_{12}^I \\ \bar{t}_{21}^I & \bar{t}_{22}^I \end{bmatrix} \begin{Bmatrix} \alpha_1^I \\ \alpha_2^I \end{Bmatrix} \tag{46}$$

Substitute the Eq. (39) into the Eqs. (45) and (46), one can obtain the particular solution writing in matrix form as

$$\mathbf{u}^p = \rho \mathbf{V} \mathbf{F}^{-1} \ddot{\mathbf{u}} \tag{47}$$

$$\mathbf{t}^p = \rho \mathbf{Q} \mathbf{F}^{-1} \ddot{\mathbf{u}} \tag{48}$$

where vector $\ddot{u}$ is the value of acceleration on each nodes, and $\mathbf{V}$ and $\mathbf{Q}$ are the matrixes of basic form of particular solution.

3.2 DHBNM

For a well-posed problem, either $\tilde{u}$ or $\tilde{t}$ is known at each node on the boundary. However, transformation between $\hat{u}_I$ and $\tilde{u}_I$, $\hat{t}_I$ and $\tilde{t}_I$ is necessary because the MLS approximation lacks the delta function property. For the panels where $\tilde{u}_I$ is prescribed, $\tilde{u}_I$ is related to $\hat{u}_I$ by zhang (2002).

$$\hat{u}_I = \sum_{J=1}^{N_t} R_{IJ} \tilde{u}_J = \sum_{J=1}^{N_t} R_{IJ} \bar{u}_J \tag{49}$$

and for the panels where $\tilde{t}_I$ is prescribed, $\hat{t}_I$ is related to $\tilde{t}_I$ by

$$\hat{t}_I = \sum_{J=1}^{N_t} R_{IJ} \tilde{t}_J = \sum_{J=1}^{N_t} R_{IJ} \bar{t}_J \tag{50}$$

where $R_{IJ} = \left[\Phi_J\left(s_I\right)\right]^{-1}$, N_t is the total number on a piece of the edge, $\bar{u}_J$ and $\bar{t}_J$ are the related nodal values.

Substituting Eqs.(47), (48), (49) and (50) into Eq. (8), then substitute the result into Eqs. (34) and (35), we can obtain

$$\mathbf{U}\mathbf{x} + \rho \mathbf{H}\mathbf{R}\mathbf{V}\mathbf{F}^{-1} \ddot{\mathbf{u}} = \mathbf{H}\mathbf{R}\bar{\mathbf{u}} \tag{51}$$

$$\mathbf{T}\mathbf{x} + \rho \mathbf{H}\mathbf{R}\mathbf{Q}\mathbf{F}^{-1} \ddot{\mathbf{u}} = \mathbf{H}\mathbf{R}\bar{\mathbf{t}} \tag{52}$$

Solving the coefficient vector x in Eq. (51), one can obtain

$$\mathbf{x} = \mathbf{U}^{-1}\mathbf{HR}\left(\mathbf{u} - \rho\mathbf{V}\mathbf{F}^{-1}\ddot{\mathbf{u}}\right) \tag{53}$$

Then Substitute Eq. (53) into Eq. (52), one can obtain

$$\mathbf{T}\mathbf{U}^{-1}\mathbf{HR}\left(\mathbf{u} - \rho\mathbf{V}\mathbf{F}^{-1}\ddot{\mathbf{u}}\right) = \mathbf{HR}\left(\mathbf{t} - \rho\mathbf{Q}\mathbf{F}^{-1}\ddot{\mathbf{u}}\right) \tag{54}$$

Eq. (54) can be rewritten as

$$\mathbf{K}\mathbf{u} - \mathbf{N}\mathbf{t} + \mathbf{M}\ddot{\mathbf{u}} = \mathbf{0} \tag{55}$$

Where

$$\mathbf{K} = \mathbf{T}\mathbf{U}^{-1}\mathbf{HR}$$

$$\mathbf{N} = \mathbf{HR}$$

$$\mathbf{M} = \rho\left(\mathbf{HRQF}^{-1} - \mathbf{T}\mathbf{U}^{-1}\mathbf{HRVF}^{-1}\right)$$

Eq. (55) is the system equation of the dual reciprocity hybrid boundary node method for dynamic analysis. The system (55) is initially partitioned according to the type of applied boundary condition, and then statically condensed in such a way that final system could be solved for unknown displacement only. Assuming that N nodes are located on the boundary, we can get N unknown variables on the boundary from Eq. (55). However, the Equation above include the displacement of the L internal nodes, and so the additional equations are needed.

3.3 Additional Equations

The Eq. (55) can not be solved for the variables of the internal nodes, additional equations for elastodynamics problem will be developed in this section.

The unknown variables of the internal nodes can be expressed as

$$u^* = u^c + u^p \tag{56}$$

The complementary solution, u^c, can be interpolated by the fundamental solution and the particular solution, u^p, can be expressed by Eq.(47). So the Eq.(56) can be rewritten as

$$\mathbf{u}^* = \mathbf{u}^s\mathbf{x} + \rho\mathbf{V}\mathbf{F}^{-1}\ddot{\mathbf{u}} \tag{57}$$

where $\mathbf{u}^*$ is the displacement of the internal nodes; $\mathbf{u}^s$ is the matrix of the fundamental solution on each internal nodes; $\mathbf{V}$ is the matrix of values of basis type of particular solution.

Substitute Eq. (53) into Eq. (57), it can be rewritten as

$$\mathbf{u}^* = \mathbf{u}^s\mathbf{U}^{-1}\mathbf{H}\mathbf{R}\mathbf{u} + \mu^2\mathbf{u}^s\mathbf{U}^{-1}\mathbf{H}\mathbf{R}\bar{\mathbf{u}}\mathbf{F}^{-1}\mathbf{u} - \mu^2\bar{\mathbf{u}}\mathbf{F}^{-1}\mathbf{u} \tag{58}$$

Rewrite Eq. (58), one can obtain

$$\mathbf{L}\mathbf{u} - \mathbf{I}\mathbf{u}_3 + \mathbf{M}_I\ddot{\mathbf{u}} = \mathbf{0} \tag{59}$$

Where I is a unit matrix.

$$\mathbf{L} = \hat{\mathbf{u}}\mathbf{U}^{-1}\mathbf{H}\mathbf{R} \tag{60}$$

$$\mathbf{M}_I = \rho\left(\mathbf{V}\mathbf{F}^{-1} - \hat{\mathbf{u}}\mathbf{U}^{-1}\mathbf{H}\mathbf{R}\mathbf{V}\mathbf{F}^{-1}\right) \tag{61}$$

The final system equations are established by combining Eqs. (55) and (59). In this paper, the Newmark time integration scheme is used. Like other hybrid models (for example, the hybrid boundary element method), the present method has a drawback of 'boundary layer effect' (the accuracy of the results in the vicinity of the boundary is very sensitive to the proximity of the interior points to the boundary). To overcome this drawback, an adaptive integration scheme has been proposed by the author. As demonstrated, the DHBNM is a boundary-only meshless approach. No boundary elements are used for both interpolation and integration purpose. The nodes in the domain are needed just for interpolation for the particular solution, which can not influence the present method as a boundary-type method.

4 Numerical Examples

In order to illustrate the validity and efficiency of the proposed method, three different examples are studied. The parameters that influence the performance of the method are also investigated. The results of the present method are compared with the analytical solutions or the solutions of dual reciprocity boundary element method (DR-BEM).

In all examples, the support size for the weight function $d_I$is taken to be $r_J = 3.5q$, with q being the average distance of adjacent nodes. And the parameter $c_I$is taken to be that $d_I/c_I = 0.5$. In this paper, $r_J = 0.85q$ is chosen as the radius of the subdomain, and the parameter c_J is taken to be $r_J/c_J = 1.1$. In order to deal with the traction discontinuities at the corners, the nodes are not arranged at these places and the support domain for interpolation is truncated.

4.1 Simply Supported Deep Beam

In this example, the simply supported deep beam with span length $L = 24$ and height $h = 6$ (see Fig.2) is considered. The beam is subjected to a Heaviside uniform load with initial value$w = 0.01$, and its material properties are: $\nu = 0.333$, $E = 100$, and $\rho = 1.5$. This problem was solved with DR-BEM using the conical $(1+r)$ function by Kontoni and Beskos (1993) and the MQ function by Samaan and Rashed (2007). Due to symmetry, a half of the beam is studied. The half beam is discretized using 60 boundary nodes and 35 internal nodes. The results for the vertical displacement history at point "A" using the DHBNM are shown in Fig.3. The results obtained by Kontoni are also plotted in the same graph. The results are almost identical which proves the validity of the present method.

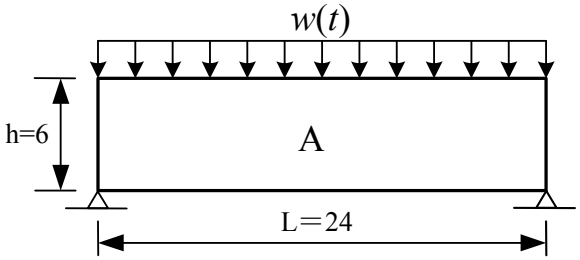

Figure 2: The simply supported beam with Heaviside load

In order to test the sensitivity of the DHBNM to the number of boundary nodes and the number of the internal nodes, different discretizations are applied. For the purpose of error estimation and convergence studies, the relative error is defined as

$$e = \frac{\left|u^{(n)} - u^{(BEM)}\right|}{u^{(BEM)}} \tag{62}$$

where the superscripts (n) and (BEM) refer to the results of DHBNM and DR-BEM. The relative errors for each nodal arrangement in DHBNM computations are presented Fig.4.

It can be concluded that the more points are arranged in the interior, the more accurate solutions can be obtained from the Fig.4. It can be observed from this figure that the present method gives very good results for this problem when more than 27 internal nodes are used.

4.2 Plate with a Hole

A rectangular plate with a hole, as shown in Fig.5, was applied a Heaviside tension load with initial value $P = 7500N/cm^2$. The material properties are: $\nu = 0.3$,

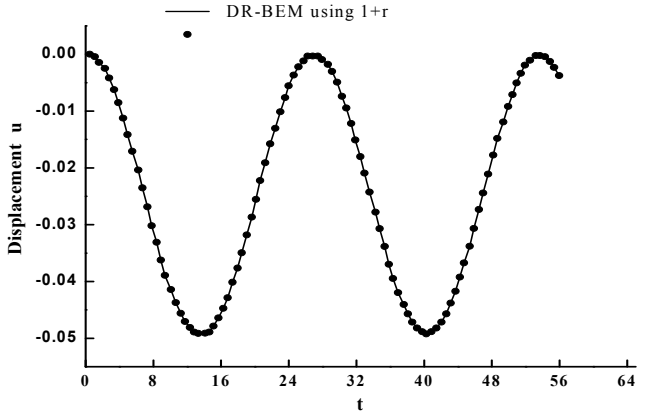

Figure 3: The dynamic vertical displacement of point A in the deep beam

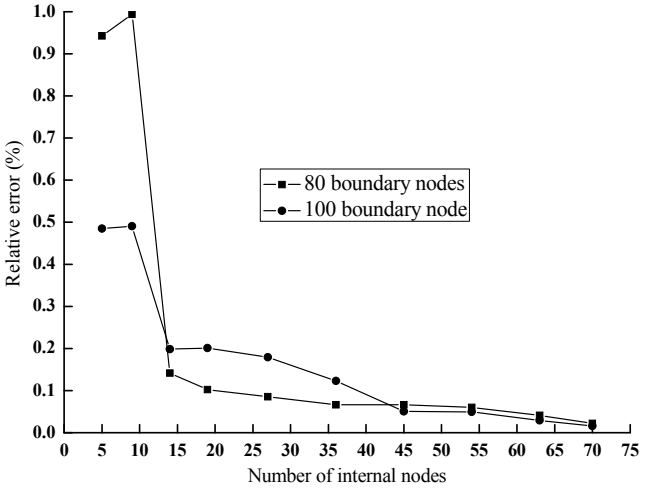

Figure 4: Relative error with different discretizations

$E = 2.1 \times 10^7 N/cm^2$, and $\rho = 0.00785 kg/m^3$, and the time step Δt is taken to be $4 \times 10^{-6} s$. One-quarter of the symmetric plate is considered. In the present calculation, the boundary of the quadrant of the plate is divided into five piecewise smooth segments (four straight lines and a quadrant arc). 40 nodes are uniformly distributed on each segment of the boundary and 40 additional internal nodes are used.

The results for the displacement history of point "A" obtained by the present method

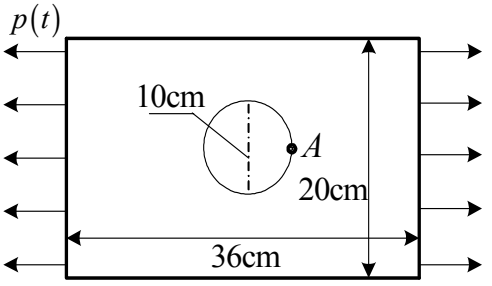

Figure 5: The gusset plate with Heaviside load

is plotted in Fig.6 and the results obtained by Agnantiaris et al. (1996) using DR-BEM are also plotted in the same graph. From the Fig.6, it can be concluded that the results of DHBNM are in excellent agreement with those of DR-BEM.

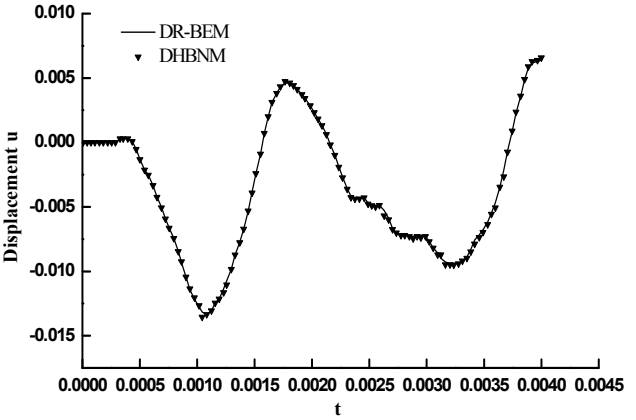

Figure 6: The history of vertical displacement of point A in the gusset plate

In order to test the sensitivity of the DHBNM to the number of boundary nodes and the number of the internal nodes, different discretizations are applied. The error estimation is defined as Eq.(62). The results with different discretization are plotted in Fig.7. From analysis, it can be concluded that the use of a number of internal nodes is important in elastodynamic problems. Based on the numerical example, with enough boundary nodes, the number of internal nodes $L = N/2$, where N is the number of the boundary nodes, provides solutions which are satisfactory for all elastodynamic problems.

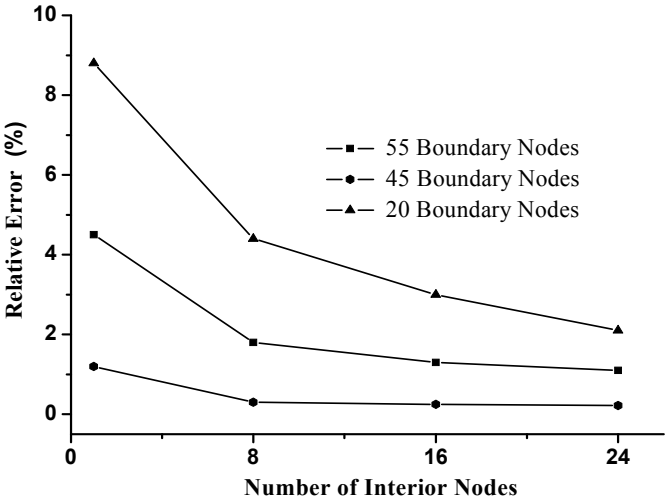

Figure 7: Relative error with different discretizations

4.3 Plate with a Central Crack

A rectangular plate with a central crack, as shown in Fig.8, is located by a step function, which is shown in Fig.9, at time $t = 0$. A state of plane stress is assumed. The dimension of the plate are: $2D = 40mm$, $2L = 20mm$. The length of the crack is $4.8mm$. First, the material is considered with elastic moduli $E = 200Mpa$, Poisson ratio $\nu = 0.3$ and density $\rho = 5000kg/m^3$. The load applied is $P(t) = 0.4Gpa$.

Due to symmetry, a quarter of the plate is studied. In the present calculation, the boundary of the quadrant of the plate is divided into five piecewise smooth segments. 60 boundary nodes and 60 internal nodes are located on the model uniformly. To simulate the singularity of the stress field on the tip of the crack, the basis function was enriched as

$$p^T(x) = \left[1,\ x,\ y,\ \sqrt{r}\right] \tag{63}$$

The Newmark method is used with $\Delta t = 1 \times 10^{-2}$ and results are computed till $t = 12\mu s$.The results of the normalized dynamic stress intensity factors for the plate with a central crack was shown in Fig.10, in which the FEM solution is also in the graph. It can be seen from the results that the DHBNM solution is close to the FEM results. Fig.11 and Fig.12 show the variation of the stress σ_x and σ_y with the distance to the tip at $t = 7\mu s$. From the results, it can be concluded that the results obtained by the present method have a good agreement with those of FEM.

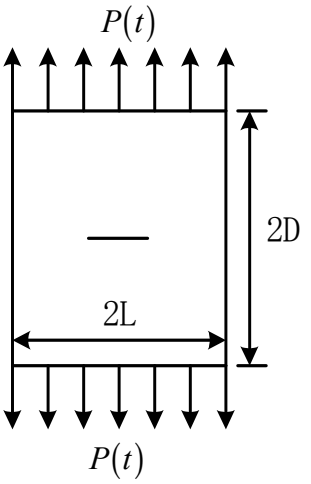

Figure 8: Plate with a central crack

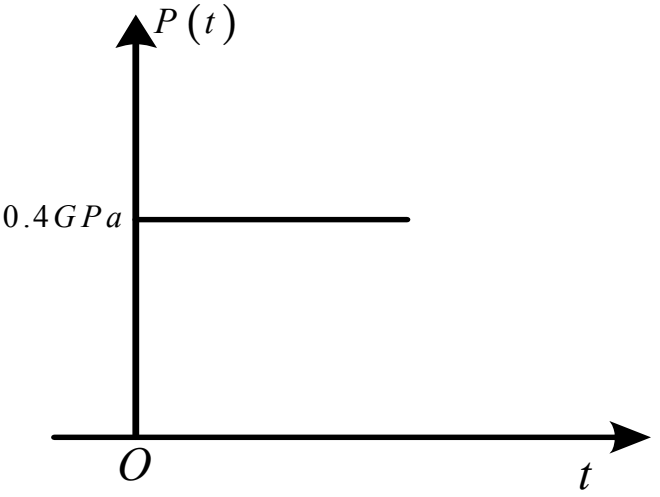

Figure 9: Step function

5 Conclusions

A truly meshless method for solving the elastodynamic problems, which called dual hybrid boundary node method (DHBNM), has been presented in this paper. This method combines the DRM and Hybrid BNM. The Hybrid BNM is used to

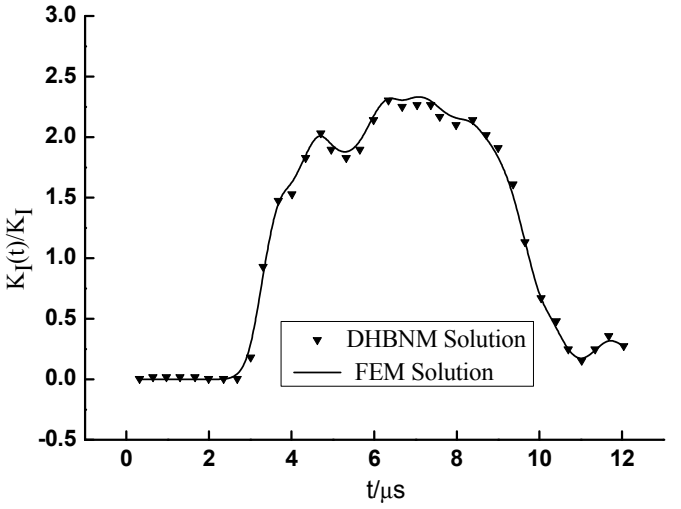

Figure 10: Regular dynamic stress intensity factor

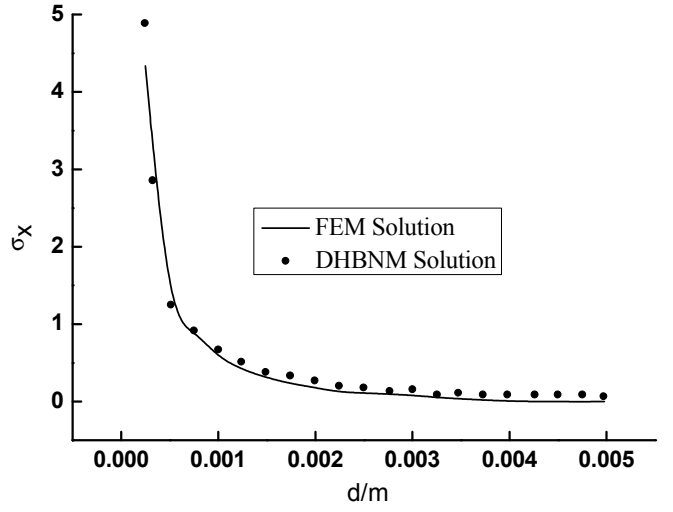

Figure 11: The variation of stress σ_x with the distance to the tip at $t = 7\mu s$

solve the homogeneous equations, while the DRM is employed to solve the inhomogeneous terms. No cells are needed either for the interpolation purposes or for integration process, only discrete nodes are constructed on the boundary of a domain, several nodes in the domain are needed just for the RBF interpolation.

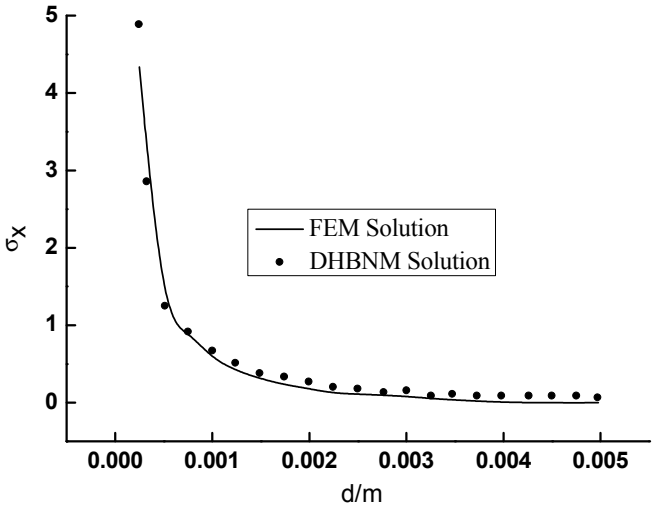

Figure 12: The variation of stress σ_y with the distance to the tip at $t = 7\mu s$

The internal nodes used in the present method are usually defined at positions where the solution is required. The use of a number of internal nodes is important in most cases. Based on the numerical examples, the number of internal node $L = \frac{N}{2}$, where N is the number of boundary nodes, provides solutions which are satisfactory for all problems.

The DHBNM has been verified and the size of the sub-domain radius is studied through the numerical examples. It is observed that the optimal value of the radius of the sub-domain is between $0.8h$ and $0.9h$.The numerical examples have been given and the numerical results have demonstrated the accuracy and convergence of the present method.

Acknowledgement: This work was supported by Natural Science Foundation of China (No. 50808090).

References

Agnantiaris, J.P., Polyzos, D., Beskos, D.E. (1996): Some studies on dual reciprocity BEM for elastodynamic analysis. *Computational Mechanics* 17, 270-277.

Aluru, N.R., Li, G. (2001): Finite cloud method: a true meshless technique based on a fixed reproducing kernel approximation. *International Journal for Numerical Methods in Engineering* 50, 2373-2410.

Atluri, S.N. (2002): *The meshless local Petrov-Galerkin (MLPG) method*. Forsyth, GA, USA, Tech Science Press.

Atluri, S.N. (2004): *The meshless method (MLPG) for domain and BIE discretizations*. Forsyth, GA, USA, Tech Science Press.

Atluri, S.N.; Han. Z.D.; Rajendran, A.M. (2004): A new implementation of the meshless finite volume method, through the MLPG "mixed" approach, *CMES: Computer Modeling in Engineering & Sciences*, vol. 6, no. 6, pp. 491-513.

Atluri, S.N.; Han. Z.D.; Shen. S.P. (2003): Meshless Local Patrov-Galerkin (MLPG) approaches for weakly-singular traction & displacement boundary integral equations, *CMES: Computer Modeling in Engineering & Sciences*, vol. 4, no. 5, pp. 507-518.

Atluri, S.N.; Shen. S.P. (2002): The meshless local Petrov-Galerkin (MLPG) method: A simple & less-costly alternative to the finite element and boundary element methods. *CMES: Computer Modeling in Engineering and Sciences*, vol. 3, no. 1, pp. 11-51.

Atluri, S.N., Zhu,T. (1998): A new meshless local Petrov–Galerkin approach in computational mechanics. *Computational Mechanics* 22, 117-127.

Atluri, S.N.; Zhu, T. (2000): New concepts in meshless methods. *International Journal of Numerical Methods in Engineering*, vol. 47, no. 1-3, pp. 537-556.

Belytschko, T., Lu, Y.Y., Gu, L. (1994): Element-free Galerkin methods. *International Journal for Numerical Methods in Engineering* 137, 229-256.

Brebbia, C.A., Dominguez, J. (1992): *Boundary Elements—An Introductory Course*, 2^{nd} ed. New York: McGraw-Hill.

Chen, H.B.; Fu, D.J.; Zhang, P.Q. (2007): An investigation of wave propagation with high wave numbers via the regularized LBIEM. *CMES: Computer Modeling in Engineering & Science*, vol. 20, no. 2, pp. 117-126.

Cheri, W., Tanaka, M. (2002): A meshless, integration-free, boundary-only RBF technique. *Computers & Mathematics with Applications* 43, 379-391.

De, S., Bathe, K.J. (2001): The method of finite spheres with improved numerical integration. *Computers & Structures* 79, 2183-2196.

Gu, Y.T., Liu, G.R. (2001): A coupled element free Galerkin/boundary element method for stress analysis of two-dimensional solids. *Computer Methods in Applied Mechanics and Engineering* 190, 4405-4419.

Kontoni, D.P.N., Beskos, D.E. (1993): Transient dynamic elastoplastic analysis by the dual reciprocity BEM. *Engineering Analysis with Boundary Element* 12, 1-16.

Lancaster, P., Salkauskas, K. (1981): Surfaces generated by moving least squares

methods. *Mathematical Computation* 37, 41-58.

Li, S.; Atluri S.N. (2008): Topology-optimization of structures based on the MLPG mixed collocation method. *CMES: Computer Modeling in Engineering & Science*, vol. 26, no. 1, pp. 61-74.

Liu, G.R., Gu, Y.T. (2001): A local point interpolation method for stress analysis of two-dimensional solids. *Structural Engineering and Mechanics* 11(2), 221-236.

Liu, G.R. (2002): *Mesh-Free Methods: Moving beyond the Finite Element Method*. Boca Raton, FL: CRC Press.

Liu, W.K., Chen, Y., Uras, R.A., Chang, C.T. (1996): Generalized multiple scale reproducing kernel particle methods. *Computer Methods in Applied Mechanics and Engineering,* 139, 91-157.

Ma, Q.W. (2007): Numerical generation of freak waves using MLPG_R and QALE-FEM methods. *CMES: Computer Modeling in Engineering & Science*, vol. 18, no. 3, pp. 223-234.

Ma, Q.W. (2008): A new meshless interpolation scheme for MLPG_R method. *CMES: Computer Modeling in Engineering & Science*, vol. 23, no. 2, pp. 75-90.

Miao, Y., Wang, Y.H., Yu, F. (2005): Development of hybrid boundary node method in two- dimensional elasticity. *Engineering Analysis with Boundary Elements* 29, 703-712.

Miao, Y., Wang, Y., Wang, Y.H. (2009): A Meshless Hybrid Boundary Node Method for Helmholtz problems. *Engineering Analysis with Boundary Element* 33(2), 120-127.

Miao, Y., Wang, Y.H. (2006): Meshless analysis for three-dimensional elasticity with singular hybrid boundary node method. *Applied Mathematics and Mechanics* 27(5), 673-681.

Miao, Y., Wang, Y.H. (2005): An improved hybrid boundary node method in two dimensional solids. *ACTA Mechanica of Solida* 18(4), 307-315.

Mukherjee, Y.X., Mukherjee, S. (1994): The boundary node method for potential problems. *International Journal for Numerical Methods in Engineering* 140, 797-815.

Nardini, D., Brebbia, C.A. (1982): A new approach to free vibration analysis using Boundary Elements, in *Boundary Element Methods in Engineering*, Computational Mechanics Publications, Southampton, and Springer-Verlag, Berlin and New York.

Nardini, D., Brebbia, C.A. (1985): Boundary integral formulation of mass matrices for dynamic analysis, in *Topics in Boundary Element Research*, Vol. 2, Springer-Verlag, Berlin and New York.

Nayroles, B., Touzot, G., Villon, P. (1992): Generalizing the finite element method: diffuse approximation and diffuse element. *Computational Mechanics* 10, 307-318.

Pini, G.; Mazzia, A.; Sartoretto, F. (2008): Accurate MLPG solution of 3D potential problems. *CMES: Computer Modeling in Engineering & Science*, vol. 36, no. 1, pp. 43-64.

Samaan, M.F., Rashed, Y.F. (2007): BEM for transient 2D elastodynamic using multiquadric functions. *International Journal of Solids and Structures* 44,8517-8531.

Sellountos, E.J.; Sequeira, A.; Polyzos, D. (2009): Elastic transient analysis with MLPG(LBIE) method and local RBFs. *CMES: Computer Modeling in Engineering & Science*, vol. 41, no. 3, pp. 215-241.

Sladek, J.; Sladek, V.; Atluri, S.N. (2001): A pure contour formulation for the meshless local boundary integral equation method in thermoelasticity. *CMES: Computer Modeling in Engineering & Science*, vol. 2, pp. 423-434.

Zhang J.M., Yao, Z.H., Li, H. (2002): A Hybrid boundary node method. *International Journal for Numerical Methods in Engineering* 53, 751-763.

Zhang J.M., Yao, Z.H., Masataka, T. (2003): The meshless regular hybrid boundary node method for 2-D linear elasticity. *Engineering Analysis with Boundary Element* 127, 259-268.

Zhu,T. (1999): A new meshless regular local boundary integral boundary integral equation approach. *International Journal for Numerical Methods in Engineering* 146, 1237-1252.

Zienkiewicz, O.C. (1977): *Finite element method.* London: McGraw-Hill.